CrossMark

Hydrogen generation behaviors of NaBH$_4$–NH$_3$BH$_3$ composite by hydrolysis

Yanmin Xu, Chaoling Wu*, Yungui Chen, Zhifen Huang, Linshan Luo, Haiwen Wu, Peipei Liu

College of Materials Science and Engineering, Sichuan University, Chengdu 610064, China

HIGHLIGHTS

- Hydrogen is generated via self-hydrolysis of NaBH$_4$-based composite (xNaBH$_4$–yNH$_3$BH$_3$) without any catalyst.
- More than 10 wt% hydrogen yield (taking reacted water into account) is achieved by optimized composition.
- The hydrolysis behaviors are affected by pH value, microstructure and the content of NH$_3$BH$_3$ in the composite.
- The detailed hydrolysis reaction processes were discussed.

ARTICLE INFO

ABSTRACT

In this work, NH$_3$BH$_3$ (AB) is used to induce hydrogen generation during NaBH$_4$ (SB) hydrolysis in order to reduce the use of catalysts, simplify the preparation process, reduce the cost and improve desorption kinetics and hydrogen capacity as well. xNaBH$_4$–yNH$_3$BH$_3$ composites are prepared by ball-milling in different proportions (from x:y = 1:1 to 8:1). The experimental results demonstrate that all composites can release more than 90% of hydrogen at 70 °C within 1 h, and their hydrogen yields can reach 9 wt% (taking reacted water into account). Among them, the composites in the proportion of 4:1 and 5:1, whose hydrogen yields reach no less than 10 wt%, show the best hydrogen generation properties. This is due to the impact of the following aspects: AB additive improves the dispersibility of SB particles, makes the composite more porous, hampers the generated metaborate from adhering to the surface of SB, and decreases the pH value of the composite during hydrolysis. The main solid byproduct of this hydrolysis system is NaBO$_2$·2H$_2$O. By hydrolytic kinetic simulation of the composites, the fitted activation energies of the complexes are between 37.2 and 45.6 kJ mol^{-1}, which are comparable to the catalytic system with some precious metals and alloys.

© 2014 Elsevier B.V. All rights reserved.

1. Introduction

Energy is the driving force of human existence and social development. As a clean fuel, hydrogen is considered to be a potential alternative energy source with the increasing serious energy crisis and growing problem of environmental pollution. However, safe and effective on-board hydrogen storage and generation remain the main issues in the hydrogen economy [1].

Among various hydrogen storage materials, sodium borohydride (NaBH$_4$, denoted as SB) and ammonia borane (NH$_3$BH$_3$, denoted as AB) are high-profile due to their high theoretical hydrogen yields (THY) of 21.3 wt% and 19.5 wt% respectively by

hydrolysis and without reacted water in calculation. Both of them belong to complex hydrides and have the following features: stable storage at ambient temperature and pressure, safe handling, ease of control for H$_2$ release [2]. There have been a lot of studies on their hydrolysis performance. SB can release hydrogen with a maximum mole ratio of H$_2$/NaBH$_4$ = 4.0 through hydrolysis and half of the hydrogen comes from H$_2$O, while AB can release hydrogen with a mole ratio of H$_2$/NH$_3$·BH$_3$ = 3.0 by hydrolysis [3]. Besides hydrogen, environmentally innocuous byproducts are produced in their hydrolysis process as well. The reactions with water can usually be described as:

$$NaBH_4 + 2H_2O \rightarrow NaBO_2 + 4H_2 \qquad (1)$$

$$NH_3BH_3 + 2H_2O \rightarrow NH_4^+ + BO_2^- + 3H_2 \qquad (2)$$
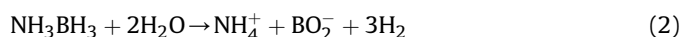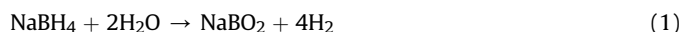
* Corresponding author. Tel./fax: +86 28 85466916.
  E-mail addresses: wuchaoling@scu.edu.cn, wmeimeiw07@163.com (C. Wu).

Eqs. (1) and (2) are the ideal stoichiometry of aqueous hydrolysis. The THY of the system AB–H$_2$O is 8.98 wt% with reacted water in calculation, which is less than that of the system SB–H$_2$O, 10.81 wt%. But in practical applications, the reactions happen always in excessive water. This point accounts for the varying degrees of hydration of the solid by-products (i.e. hydrated metaborates) [4]. Hence, we characterize the hydrolysis by-products through XRD in order to discover the actual reaction process of the composites.

Low hydrogen productivity of either SB or AB at room temperature is regarded as a key barrier to their commercialization [5]. Catalytic hydrolysis accelerates hydrogen generation rate and achieves on-demand hydrogen production by controlling the contact of catalyst with aqueous solution [6]. Published literature has explored various catalysts such as noble [7–9] or non-noble metals [10,11], alloys [12–16] and acids [17,18]. At the same time, the following points have to be considered for practical applications: the low hydrogen yield caused by non-hydrolyzable catalysts, the high cost of noble metals, the relatively complex preparation process of some metal catalysts and alloys, corrosion resistance and long-term cyclic stability [11]. Besides the use of catalysts, there is also some research focusing on hydrolysis of solid SB with steam/water vapor at high temperatures [4]. Nevertheless, the operating conditions still need to be optimized.

In this work, a new approach is introduced for hydrogen generation, which uses AB with high hydrogen yield to induce the hydrolysis of SB with high hydrogen yield as well and does not require any other catalyst in the reaction process. The SB-based composites xSB–yAB used in this work were prepared simply and conveniently. These composites exhibited much higher hydrogen generation yields and better hydrolysis properties than pure SB or pure AB. The hydrolysis kinetics of the composites and the inducing mechanism of AB are discussed in various aspects, such as the change of activation energies, the evolution of pH values, etc.

2. Experimental

2.1. Sample preparation

In our experiments, NaBH$_4$ (SB, 99%) is used as received. NH$_3$BH$_3$ (AB) is synthesized by the procedure mentioned in the literature [19] and the purity is about 90%. All raw materials are stored and all manipulations are carried out in an argon glove box with <5 ppm O$_2$ and <10 ppm H$_2$O. An SPEX8000 high-energy ball miller is employed to prepare for xNaBH$_4$–yNH$_3$BH$_3$ composite samples in different x:y molar ratios ranged from 1:1 to 8:1 and with the ball-to-powder weight ratio of 30:1 under Ar atmosphere for 15 min.

2.2. Hydrolysis test

An experimental apparatus is designed to monitor the hydrogen generation amount/rate from the xSB–yAB composites, as was described in Ref. [20]. Predetermined quantity of the composites (0.2 g) is weighted in an argon-filled glove box and then transferred into a 250 ml round-bottom flask sealed by a dual-port tube with one water inlet plug and one hydrogen outlet plug. 10 ml water is injected into the flask through syringe pump, and the reaction is started by stirring the contents at different temperatures (25, 40, 50, 60 and 70 °C). The evolution of gas goes through CuSO$_4$ solution, a condenser and a dry tube with CaCl$_2$, respectively. These procedures aim at absorbing ammonia in the gas stream, separating steam emitted from the reaction and drying the gas, respectively. At last, the generated hydrogen is collected and measured in an inverted 1.5 L graduated cylinder immersed in a water-filled tray. The residual solution is immediately dried in a vacuum oven after

reaction to obtain byproducts. Each experiment is performed twice in order to ensure the accuracy of the results.

2.3. Microstructure analysis

Powder X-ray diffraction (XRD) is used for characterizing the crystalline structure of the milled composite samples and the hydrolysis byproducts. The patterns are recorded on a DX-2600 diffractometer with CuKα radiation. The morphologies of the milled samples are detected by scanning electronic microscope (SEM), which is performed on a JSM-7500F scanning electron microscope.

3. Results and discussion

3.1. Hydrolysis performance of SB-AB composites and monomers

Fig. 1a reveals hydrogen generation curves of 4SB–AB composite in 1 h, and it's obviously seen that the chemical reaction rate is affected by temperature significantly. The higher the temperature, the quicker the hydrogen evolution rate, and the higher the hydrogen yield (note: the hydrogen yield mentioned in this work is considered for 1 h only). The H$_2$ yield increases from 3.28 wt% up to 10.41 wt% when the temperature rises from 25 to 70 °C, and the H$_2$ yield at 70 °C almost close to complete theoretical dehydrogenation. By contrast, the hydrolysis property of pure SB or pure AB is poor, as shown in Fig. 1b and c. The H$_2$ yields of the above monomers are lower than those of the composites at the same temperatures in the same time. Pure SB releases about 2.17 wt% and 8.86 wt% at 25 °C and 70 °C in 1 h, respectively. Pure AB only generates 0.63 wt% H$_2$ at 25 °C, and even at 70 °C, the highest H$_2$ amount is only 1.89 wt%, which is far less than the THY of 8.98 wt%.

The H$_2$ yields of xNaBH$_4$–yNH$_3$BH$_3$ composites at different temperatures can be seen in Table 1. As shown in both Fig. 1 and Table 1, it is obvious that the dehydrogenation property of the composites is superior to both pure AB and pure SB at any temperature, especially above 40 °C. It is demonstrated that the combination of the two compounds gives a synergetic effect. Meanwhile, the temperature has great effects on hydrolysis behaviors of these composites, and the mechanism is discussed in details in Section 3.3.1.

Aside from the temperature effect, the H$_2$ yield is also affected by the molar ratio of SB to AB. Fig. 2 shows the hydrogen release behaviors of a series of xSB–yAB composites by hydrolysis with magnetic stirring at 60 °C. All the curves have the same variation trend: there is a very fast reaction rate in the initial 10 min and then the rate slows down with the reaction proceeding. All composites can generate more than 3 wt% H$_2$ in 5 min, then continue to produce about 2 wt% more H$_2$ in 10 min. The amount of H$_2$ released in the first 10 min almost accounts for half of total H$_2$ yield in 1 h. The theoretical hydrogen yield of the composites increases with the rise of SB content (Table 1). However, the experimental results show that with the increase of the SB concentration from SB–AB to 8SB–AB, the actual H$_2$ yield increases first and then decreases. 4SB–AB and 5SB–AB have the highest H$_2$ yields of 9.42 wt% and 9.45 wt% respectively. The kinetics data of all xSB–yAB composites at different temperatures have the similar variation trend. Therefore, we only show the kinetics data for one temperature. More detailed information about the hydrolysis curves of each composite at other temperatures (25, 40, 50, and 70 °C) can be found in Fig. S1 in Supplementary data.

3.2. Analysis of SB-AB composites and hydrolysis by-products

Fig. 3 shows the XRD patterns of xSB–yAB composites with various molar ratios after ball milling under Ar atmosphere for
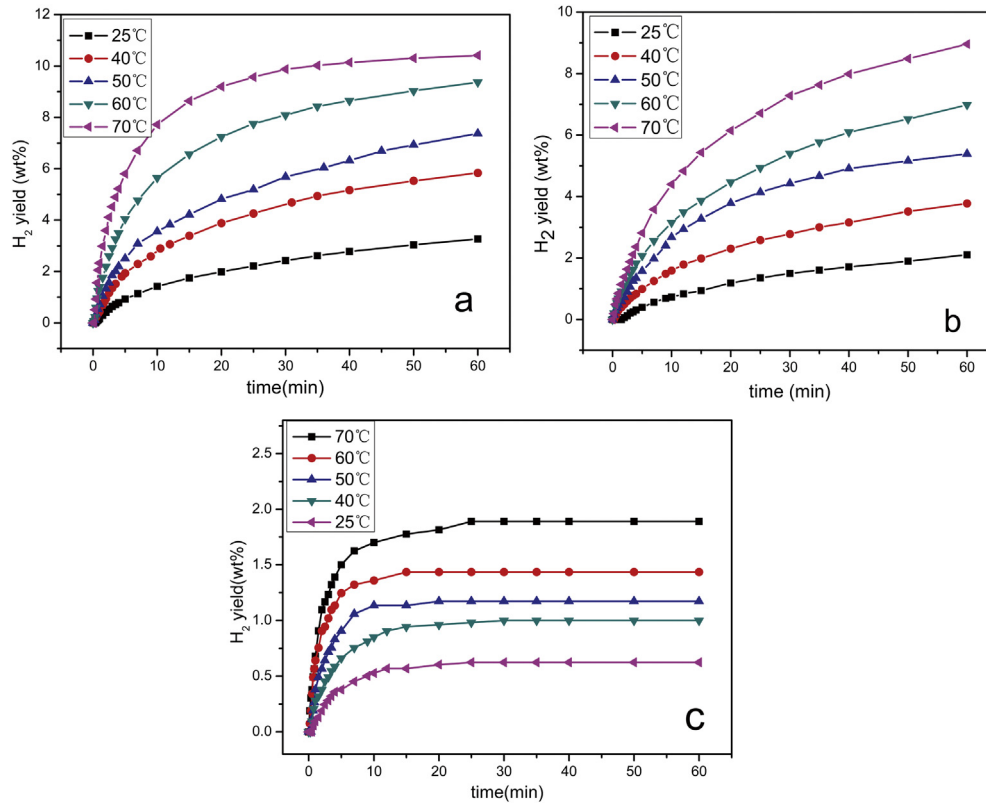
Fig. 1. Hydrolysis curves of: (a) 4SB–AB composite; (b) SB; (c) AB under different temperatures.

15 min. As is shown in Fig. 3, the main phases of the composites are still $NaBH_4$ and NH_3BH_3, and no new phases are detected. It indicates that there is no chemical reaction between SB and AB during the high-energy milling process.

Morphology and surface chemistry of the solid composites prepared by high-energy ball milling are examined by SEM with EDS. As can be seen from Fig. 4, the particle size of the composite significantly decreases after ball milling with an average size of 1–4 μm. Little AB was seen in SEM micrographs of 8SB-AB, for the AB content is low, and AB has a strong water-absorption ability. Thus, AB changes into amorphous morphology, and covers the surface of SB crystal particles. AB additive plays an important role in preventing SB particle agglomeration, making the composite more porous and moreover, improving the dispersion of SB particles. These factors help to increase the specific surface area of the

composite and maximize the contact with water during hydrolysis. Moreover, to some extent, AB distributing around SB hampers the generated metaborate from adhering to the surface of SB, and promote the hydrolysis of SB more thoroughly and hydrogen generation more effectively.

Fig. 5 illustrates XRD patterns acquired from the solid by-products after the hydrolysis of xSB–yAB composites. The main by-product phase is hydrated sodium metaborate $NaBO_2 \cdot 2H_2O$ (ICDD ref. 06-0122). NH_3 is detected by precipitates formed in $CuSO_4$ solution during the experiment, which is known as one of

Table 1
The H_2 yields (wt%) of xNaBH$_4$–yNH$_3$BH$_3$ composites[a,b]

H_2 yield (wt%)						
x:y	25 °C	40 °C	50 °C	60 °C	70 °C	Theoretical hydrogen yield
Pure SB	2.17	3.92	5.83	7.02	8.86	10.81
Pure AB	0.63	1.00	1.19	1.43	1.89	8.98
1:1	2.80	5.22	6.53	7.85	9.32	10.00
2:1	3.01	5.38	6.92	8.37	9.61	10.33
3:1	3.11	5.48	7.11	9.05	9.89	10.41
4:1	3.28	5.84	7.33	9.42	10.41	10.49
5:1	3.20	5.69	6.87	9.45	10.44	10.55
6:1	2.50	5.47	6.62	9.28	9.77	10.58
7:1	2.78	5.13	6.80	9.30	9.73	10.61
8:1	2.69	5.07	6.62	9.20	9.64	10.63

[a] The theoretical hydrogen yield is calculated in accordance with Eqs. (1) and (2).
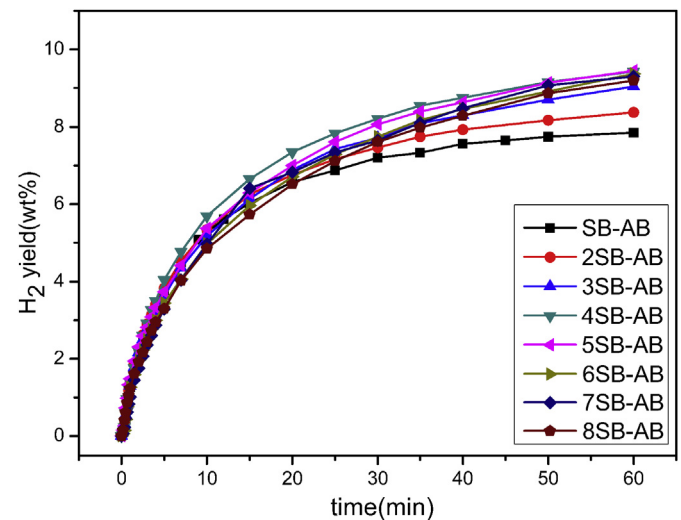[b] The yields of composites at different temperatures are considered for 1 h only.

Fig. 2. The hydrolysis curves of different xSB–yAB composites at 60 °C.

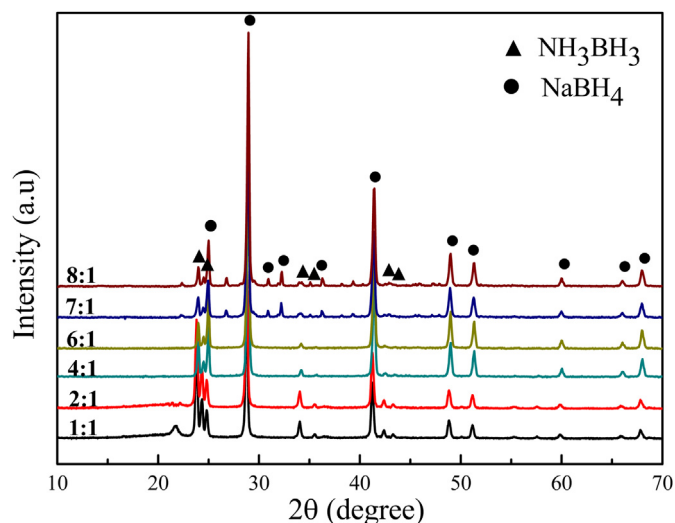**Fig. 3.** XRD patterns of xSB–yAB composites in different molar ratios (x:y = 1:1, 2:1, 4:1, 6:1, 7:1, 8:1) after ball-milling for 15 min.

Fig. 5. XRD patterns of the by-products after the hydrolysis of xSB–yAB composites at 40 °C.

hydrolysis by-products of AB [21]. And sodium metaborate is observed as the main solid by-product of SB hydrolysis in many former studies.

Furthermore, XRD results show that the hydrolysis by-products are affected little by the reaction temperature. The main by-product is $NaBO_2 \cdot 2H_2O$ within the experimental temperature range. However, Andrieux et al. [22] mentioned in their work that temperature affected the phase formed by $NaBH_4$ hydrolysis, i.e. the hydration degree of borate compound, which is in contrast to the result in this work.

Fig. 6 represents the XRD patterns of the hydrolysis by-products exposed to air for 2 months. Upon prolonged exposure to air, the
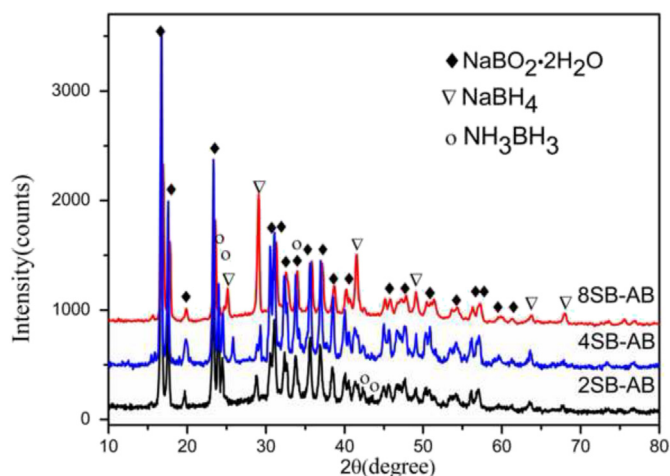
main by-product $NaBO_2 \cdot 2H_2O$ and unreacted SB finally transform to the sodium tetraborate pentahydrate $Na_2B_4O_7 \cdot 5H_2O$ (ICDD ref. 07-0277), which is also consistent with the result in Ref. [23]. It can be explained that the observed phase transition as hydration of the by-product is due to air moisture.

3.3. Hydrolysis mechanism

3.3.1. Influence of temperature on hydrolysis properties
As described in Section 3.1, xSB–yAB composites show improved hydrolysis kinetics and higher hydrogen generation yield compared with pure SB or pure AB. Their hydrogen generation performances at higher temperature make them attractive particularly for practical applications. The improvement mainly
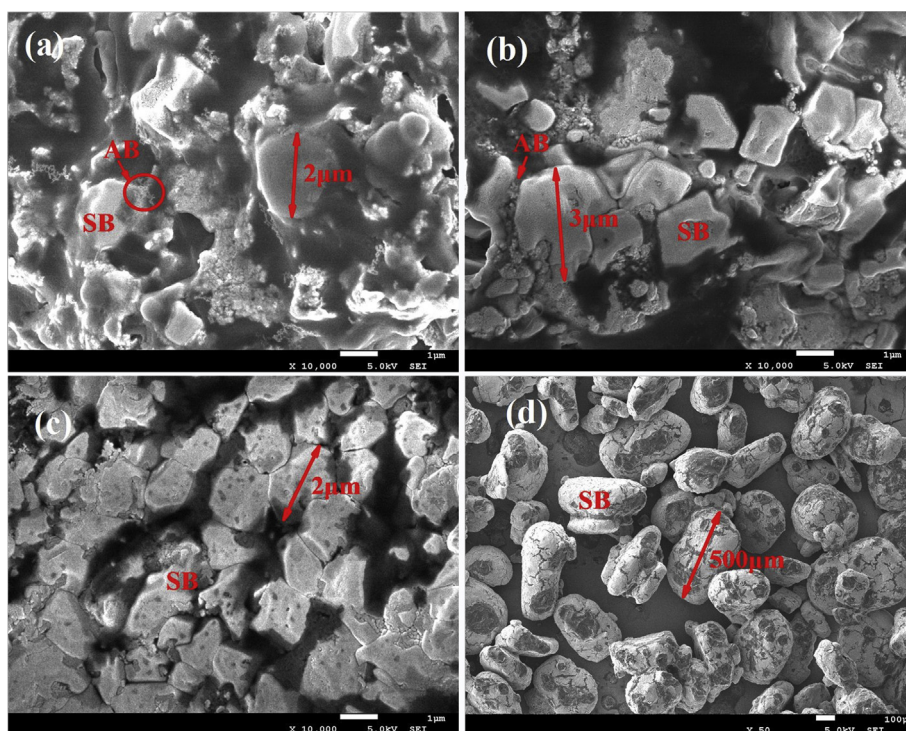

Fig. 4. SEM micrographs of the samples before hydrolysis: (a) SB–AB; (b) 4SB–AB; (c) 8SB–AB; (d) pure SB without ball milling.
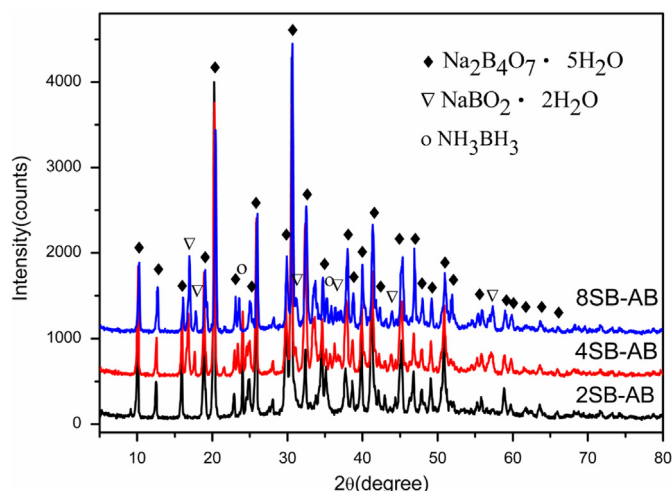
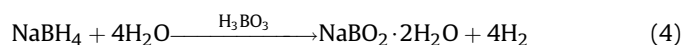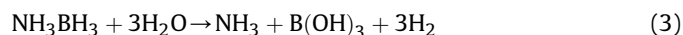**Fig. 6.** XRD patterns of the solid by-products exposed to air for 2 months.

comes from the following factors: firstly, the processes of dissolving AB and SB in water are endothermic [21,24], and thus higher temperature favors the dissolution of the composite, which is an important step in the hydrolysis process [25]. Secondly, the dynamic activity of the particles (i.e. the movement and the collision of particles) in solution improves with increased temperature, leading to an easier hydrolysis start and subsequent hydrogen release.

3.3.2. Evolution of the aqueous solution pH values

Schlesinger et al. [26] found that the solution pH value was one of the limiting parameters for the hydrolysis of SB. Accordingly, the evolution of the solution pH values for some samples is then monitored. The pH value of the solution in reactions is 8.8–11.2, which shows weakly alkaline. As shown in Fig. 7a, pH value rises up to 11.20 from 10.40 when the temperature rises from 25 °C to 70 °C. The pH value of the resulting solution from SB hydrolysis increases since the BH_4^- anions converted into alkaline ions BO_2^-. The higher the temperature, the more thorough the conversion. However, it is clear that the alkalinity has a negative effect on H_2 generation yield of SB hydrolysis, and the increasing pH value leads to the decrease in initial hydrogen evolution rate. Adding AB decreases the pH value of the composite. At 60 °C, the pH value of the solution after hydrolysis is less than that of pure SB, as shown in Fig. 7b, and with the increase of the amount of AB, the pH value decreases. On one hand, AB is added to reduce the amount of SB in composite, which also led to a decline in BH_4^- ions concentration. On the other hand, boric acid as a kind of weak acid produced during the hydrolysis of AB can reduce the pH value of the solution. Thereby, the hydrogen generation property of the composite outperforms its monomers.

3.3.3. Reaction route

According to the detected by-products of composite and many former studies [25,27,28] about the hydrolysis procedure of SB and AB, the composite hydrolysis reactions are concluded as follows:

$$NH_3BH_3 + 3H_2O \rightarrow NH_3 + B(OH)_3 + 3H_2 \qquad (3)$$

$$NaBH_4 + 4H_2O \xrightarrow{\quad H_3BO_3 \quad} NaBO_2 \cdot 2H_2O + 4H_2 \qquad (4)$$

However, we cannot infer that AB and SB hydrolyze respectively in the process of the composite hydrolysis. The detailed reacting process is suggested as follows:
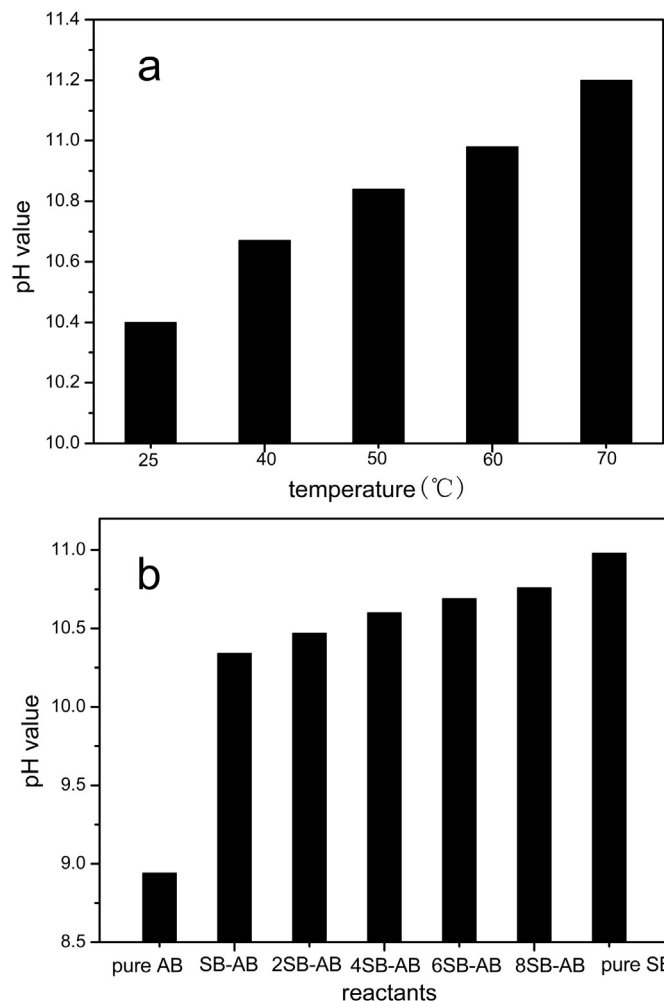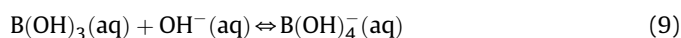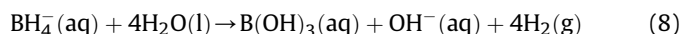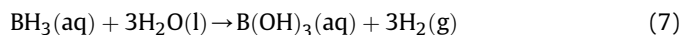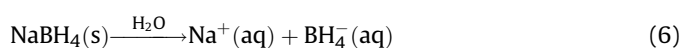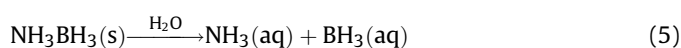

Fig. 7. The pH values of the resulting solution after hydrolysis: (a) pure SB at different temperatures; (b) different reactants at 60 °C.

$$NH_3BH_3(s) \xrightarrow{\quad H_2O \quad} NH_3(aq) + BH_3(aq) \qquad (5)$$

$$NaBH_4(s) \xrightarrow{\quad H_2O \quad} Na^+(aq) + BH_4^-(aq) \qquad (6)$$

$$BH_3(aq) + 3H_2O(l) \rightarrow B(OH)_3(aq) + 3H_2(g) \qquad (7)$$

$$BH_4^-(aq) + 4H_2O(l) \rightarrow B(OH)_3(aq) + OH^-(aq) + 4H_2(g) \qquad (8)$$

$$B(OH)_3(aq) + OH^-(aq) \Leftrightarrow B(OH)_4^-(aq) \qquad (9)$$

According to the calculated results in Ref. [29], the B–N bond distance (1.666 Å) in AB is longer than either that of B–H (1.208 Å) or N–H (1.071 Å), reflecting that B–N bond is easier to be broken than the other two bonds in AB. After high-energy ball milling, the activity of the composite powder increases. It is reasonable to consider that there are some interactions between AB and SB molecules. In the joint function of H_2O molecules and the electron-donating group BH_4^-, the B–N bond is broken and AB is decomposed into BH_3 and NH_3, as shown in Eq. (5) [20]. A solvated form of BH_3 is proposed as a highly reactive intermediate which is converted to product boric acid along with the H_2 release via a series of rapid steps [28]. In return, the electron donor NH_3 and the electron acceptor BH_3 provided by AB have an impact on the electron

configuration of BH_4^-, causing B–H bond in $BH_4^{-^-}$ more unstable and easier dehydrogenated. The increase in pH value during reaction can be explained by Eq. (7) which occurs in a stepwise manner [25]. But in an alkaline environment, boric acid generated by reactions (7) and (8) will continue to react with OH^- ions and convert to $B(OH)_4^-$ ultimately. Based on this reason, boric acid is not detected by XRD patterns.

3.3.4. Reaction activation energy of xSB–yAB system

The hydrolysis reaction kinetics of xSB–yAB composite is further investigated at varied temperatures. The obtained kinetic simulation curves of 4SB–AB composites are presented in Fig. 8. As shown in Fig. 8a, H_2 generation is expressed as conversion rate (%), which is defined by the volume of produced H_2 over the theoretical volume of H_2, and all composites were assumed to react completely. The simulation curves are found to be well fitted to the Avrami equation (Eq. (10)), which is deduced from the nucleation and growth process:

$$F(t) = 1 - \exp(-kt^m) \tag{10}$$

where F is the reaction rate; k is reaction constant; m is Avrami constant; and t is reaction time. The values of k and m can be obtained by fitting. The values of the constants for the Avrami equations derived from all the composites and the R^2 values can be found in Table S1 in Supplementary data. The correlation factor (R^2)

of each curve for the hydrolysis of 4SB–AB composite exceeds 0.99, the similar characteristics can be found for the other xSB–yAB composites and pure SB, but not for pure AB. This result confirms that the hydrolysis reactions of xSB–yAB composites obey the nucleation and growth mechanism, which is in agreement with the study by L.Z. Ouyang et al. [30].

According to Arrhenius equation, the reaction rate constant and temperature exhibit exponential relationship:

$$k = A \exp(-E_a/RT) \tag{11}$$

where k is the reaction rate constant (in this work, k was obtained from formula (10)), T is the reaction temperature, A is the pre-exponential factor and R is the universal gas constant, and E_a is the activation energy. Eq. (11) can be written as:

$$\ln k = \ln A - (E_a/R) \cdot (1/T) \tag{12}$$

An Arrhenius plot of $\ln k$ (reaction constant) versus the reciprocal of absolute temperature ($1/T$) is shown in Fig. 8b. From the slope of the fitted straight line, the activation energy of the hydrolysis reaction is calculated to be 37.23 kJ mol^{-1} and the correlation factor (R^2) value is more than 0.99. Arrhenius plots for other composites and the R^2 values can be found in Fig. S2 in Supplementary data.

Table 2 shows the activation energies of different mole ratio of xSB–yAB composites. The corresponding results are in the range of 30–90 kJ mol^{-1} in metal catalyzed hydrolysis of sodium borohydride, ammonia borane, and ammonia triborane [31], and close to the results reported for the hydrolysis of $NaBH_4$ catalyzed by Pt–$LiCoO_2$ (35.75 kJ mol^{-1}) [32], Co (41.9 kJ mol^{-1}) [33], Ru(0) nanoclusters (43 kJ mol^{-1}) [34], Ni_xB (38 kJ mol^{-1}) [35] and Co–P–B on Ni foam (38.8 kJ mol^{-1}) [36]. It indicates that catalyst-free xSB–yAB composites have good kinetics property as those with catalysts. As can be seen from the results, from $x/y = 1$ to $x/y = 4$, the activation energy decreases, and from $x/y = 4$ to $x/y = 8$, the activation energy increases. Among them, 3SB–AB, 4SB–AB and 5SB–AB composites have the lower activation energies. This is consistent with the result that these composites have the better comprehensive properties as seen in Fig. 2.

4. Conclusions

The xSB–yAB composites have been prepared by a mechanical milling method. Both the hydrolysis property and the reaction mechanism of the composites are studied. The main conclusions are as follows:

1) Without any catalyst, the xSB–yAB composites (molar ratios ranging from 1:1 to 8:1) show much better hydrolysis kinetics and higher hydrogen generation yields compared with pure SB or AB. All composites release above 90% of hydrogen in an hour at 70 °C and their hydrogen yields reach 9 wt% even taking the reacted water into account.

2) The H_2 generation yield reaches 99% when the molar ratio of SB/AB is 4:1 or 5:1. And the corresponding mass hydrogen production is over 10 wt%, indicating that the xSB–yAB composites maybe promising materials to produce hydrogen for practical application.

Fig. 8. Hydrolysis kinetics simulation curves of 4SB-AB composite.

Table 2
The activation energies of xSB–yAB composites.

x:y	1:1	2:1	3:1	4:1	5:1	6:1	7:1	8:1	SB
E_a (kJ mol^{-1})	45.59	42.27	38.70	37.23	38.34	42.8	43.78	44.12	40.07

3) The main solid hydrolysis by-product of the composites is $NaBO_2 \cdot 2H_2O$, and it transforms into $Na_2B_4O_7 \cdot 5H_2O$ when exposed to air for 2 months. This phase transition is due to air moisture.

4) The improvements of the hydrolysis properties of the xSB–yAB composites may be attributed to the following factors: a). The addition of AB improves the dispersibility of SB particles and increases the specific surface area of the composites; b). AB distributing around SB hampers the generated metaborate from adhering to the surface of SB, and promote the hydrolysis of SB more thoroughly; c). Adding AB decreases the pH values of the solutions during hydrolysis; d). The combination of the two compounds gives a synergetic effect in the reacting process.

5) Catalyst-free xSB–yAB composites have good kinetics property as those with catalysts. The activation energies of a series of xSB–yAB composites are in the range of 37.2–45.6 kJ mol^{-1}, which are comparable to the catalytic $NaBH_4$ with some precious metals and alloys.

Appendix A. Supplementary data

Supplementary data related to this article can be found at http://dx.doi.org/10.1016/j.jpowsour.2014.03.038.

References

[1] L. Schlapbach, A. Züttel, Nature 414 (2001) 353–358.
[2] T. Umegaki, J.-M. Yan, X.-B. Zhang, H. Shioyama, N. Kuriyama, Q. Xu, Int. J. Hydrogen Energy 34 (2009) 2303–2311.
[3] M. Yadav, Q. Xu, Energy Environ. Sci. 5 (2012) 9698–9725.
[4] E. Marreroalfonso, J. Gray, T. Davis, M. Matthews, Int. J. Hydrogen Energy 32 (2007) 4717–4722.
[5] J.-H. Kim, K.-H. Choi, Y.S. Choi, Int. J. Hydrogen Energy 35 (2010) 4015–4019.
[6] B.H. Liu, Z.P. Li, J. Power Sources 187 (2009) 527–534.
[7] C. Crisafulli, S. Scirè, M. Salanitri, R. Zito, S. Calamia, Int. J. Hydrogen Energy 36 (2011) 3817–3826.
[8] N. Patel, B. Patton, C. Zanchetta, R. Fernandes, G. Guella, A. Kale, Int. J. Hydrogen Energy 33 (2008) 287–292.
[9] M. Chandra, Q. Xu, J. Power Sources 168 (2007) 135–142.
[10] Q. Xu, M. Chandra, J. Power Sources 163 (2006) 364–370.
[11] S.S. Muir, X. Yao, Int. J. Hydrogen Energy 36 (2011) 5983–5997.
[12] L. Soler, J. Macanas, M. Munoz, J. Casado, Int. J. Hydrogen Energy 32 (2007) 4702–4710.
[13] C.-H. Liu, B.-H. Chen, C.-L. Hsueh, J.-R. Ku, M.-S. Jeng, F. Tsau, Int. J. Hydrogen Energy 34 (2009) 2153–2163.
[14] M. Nie, Y.C. Zou, Y.M. Huang, J.Q. Wang, Int. J. Hydrogen Energy 37 (2012) 1568–1576.
[15] A.A. Vernekar, S.T. Bugde, S. Tilve, Int. J. Hydrogen Energy 37 (2012) 327–334.
[16] M.-q. Fan, S. Liu, L.-X. Sun, F. Xu, S. Wang, J. Zhang, D.-s. Mei, F.-l. Huang, Q.-m. Zhang, Int. J. Hydrogen Energy 37 (2012) 4571–4579.
[17] M. Chandra, Q. Xu, J. Power Sources 159 (2006) 855–860.
[18] C.M. Kaufman, B. Sen, J. Chem. Soc., Dalton Trans. (1985) 307–313.
[19] P.V. Ramachandran, P.D. Gagare, Inorg. Chem. 46 (2007) 7810–7817.
[20] Z.F. Huang, C.L. Wu, Y.G. Chen, X.L. Wang, Int. J. Hydrogen Energy 37 (2012) 5137–5142.
[21] J. Baumann, Physikalisch-chemische untersuchungen zur wasserstoffabgabe von BNH-verbindungen, Doctoral thesis, Technische Universität Bergakademie Freiberg, Institut für Physikalische Chemie, 2003.
[22] J. Andrieux, L. Laversenne, O. Krol, R. Chiriac, Z. Bouajila, R. Tenu, J.J. Counioux, C. Goutaudier, Int. J. Hydrogen Energy 37 (2012) 5798–5810.
[23] N. Stepanov, V. Uvarov, I. Popov, Y. Sasson, Int. J. Hydrogen Energy 33 (2008) 7378–7384.
[24] L. Damjanović, S. Bennici, A. Auroux, J. Power Sources 195 (2010) 3284–3292.
[25] A. Gonçalves, P. Castro, A. Novais, Chem. Eng. Trans. 12 (2007) 243–248.
[26] H.I. Schlesinger, H.C. Brown, A.B. Finholt, J.R. Gilbreath, H.R. Hockstra, E.K. Hyde, J. Am. Chem. Soc. 75 (1953) 215–219.
[27] R.E. Davis, E. Bromel, C.L. Kibby, J. Am. Chem. Soc. 84 (1962) 885–892.
[28] H.C. Kelly, V.B. Marriott, Inorg. Chem. 18 (1979) 2875–2878.
[29] Y. Meng, Z. Zhou, C. Duan, B. Wang, Q. Zhong, J. Mol. Struct. (THEOCHEM) 713 (2005) 135–144.
[30] L.Z. Ouyang, Y.J. Xu, H.W. Dong, L.X. Sun, M. Zhu, Int. J. Hydrogen Energy 34 (2009) 9671–9676.
[31] S. Karahan, M. Zahmakıran, S. Özkar, Int. J. Hydrogen Energy 36 (2011) 4958–4966.
[32] Z. Liu, B. Guo, S.H. Chan, E.H. Tang, L. Hong, J. Power Sources 176 (2008) 306–311.
[33] B.H. Liu, Z.P. Li, S. Suda, J. Alloys Compd. 415 (2006) 288–293.
[34] M. Zahmakıran, S. Özkar, J. Mol. Catal. A: Chem. 258 (2006) 95–103.
[35] H. Dong, H. Yang, X.P. Ai, C. Cha, Int. J. Hydrogen Energy 28 (2003) 1095–1100.
[36] N. Patel, A. Kale, A. Miotello, Appl. Catal., B 111–112 (2012) 178–184.